Cogging Torque Reduction of Interior Permanent-Magnet Synchronous Motors by Finite-Element Method

Yi-Chang Wu[1], Wan-Tsun Tseng[2] and Pei-Li Tsai[3]
[1, 3] Department of Mechanical Engineering, National Yunlin University of Science & Technology, Yunlin, Taiwan 640, R.O.C.
[2] Department of Electrical Engineering, National Yunlin University of Science & Technology, Yunlin, Taiwan 640, R.O.C.

E-mail: wuyc@yuntech.edu.tw

Abstract. The cogging torque of a permanent-magnet motor is an oscillatory torque that always induces vibration, acoustic noise, possible resonance and speed ripples, and its minimization is a major concern for electric motor designers. This paper presents an effective approach for the cogging torque reduction of interior permanent-magnet motors by modifying the magnet span angle of the rotor and the shoe depth and shoe ramp of the stator. The cogging torque is calculated by employing a commercial finite-element analysis software Ansoft/Maxwell. The results show that the peak value of the cogging torque for the modified design decreases 50% in comparison with that of the original design.

1. Introduction

An electric motor is an electric device that converts electrical energy into mechanical energy. Among various types of electric motors, interior permanent-magnet (IPM) synchronous motors have attracted extensive interest due to the characteristics of high efficiency, high torque-to-volume ratio, low cost of maintenance and a long constant power operating range [1]. IPM synchronous motors generate not only electromagnetic torque but also reluctance torque by the rotor saliency, so they are widely used in traction motors of electric and hybrid vehicles and electrical power steering systems of automobiles. However, the IPM synchronous motor possesses an inherent cogging torque that causes the torque ripple as well as prevents a smooth rotation. The cogging torque is an oscillatory torque that always induces vibration, acoustic noise, possible resonance, speed ripples, and position inaccuracy, which is detrimental to the motor performance particularly at light load and low speed. Therefore, the reduction of the cogging torque becomes a major concern for electric motor designers. Several approaches have been developed to attempt minimizing the cogging torque of permanent-magnet motors, such as stepped skewing of permanent-magnet blocks [2], modifying permanent magnet arc [3, 4], providing different magnet widths [1], and shifting the pole pairs by half a slot pitch [5], etc. However, these methods are not available for IPM synchronous motors due to buried permanent magnets and geometric constraints of rotors. In this paper, an exterior-rotor IPM synchronous motor is introduced, and the effects of design parameters of the rotor and stator on the cogging torque are discussed by finite-element analysis.

2. An exterior-rotor IPM synchronous motor

For an exterior-rotor IPM synchronous motor, permanent magnets with even numbers are buried inside the rotor, while the stator with fixed polyphase windings appears on the inside of the rotor. Figure 1 shows a cross-sectional view of a 3-phase, 12-pole/18-slot IPM synchronous motor with a one-layer V-shape rotor topology. Such a kind of IPM motor has been widely used in electrical vehicles. The rotor is formed by laminating steel plates including magnetic barriers and magnet insertion holes in which permanent magnets are buried. The variation of the reluctance around the

---

[1] To whom any correspondence should be addressed.

rotor creates saliency in the rotor structure of an IPM synchronous motor. Therefore, the IPM rotor generates reluctance torque in addition to electromagnetic torque due to magnetic saliency.

3. Cogging torque analysis

By definition, no stator current excitation is involved in the cogging torque production. The cogging torque directly arises from the mutual interaction of permanent magnets and the stator slotted structure of the IPM motor as the rotor rotates relative to the stator. Therefore, it is greatly affected by the configurations and dimensions of the rotor and stator. In this section, the effects of several design parameters, including the magnet span angle α of the rotor, the shoe depth d_1 and the shoe ramp d_2 of the stator, on the cogging torque are discussed by finite-element analysis. Figure 2 shows geometric parameters of the exterior-rotor IPM synchronous motor. The corresponding values of the magnetic properties and geometrical dimensions are given in table 1. The Ansoft/Maxwell 2D field simulator is employed to the cogging torque analysis of the two-dimensional IPM motor configuration. The period of the cogging torque for this IPM motor is $360°/\text{lcm}(P, S)= 360°/\text{lcm}(12, 18)=360°/36=10°$. The symbol P is the number of magnet poles, the symbol S is the number of stator slots, and $\text{lcm}(P, S)$ is the least common multiplier between P and S. The computed cogging torque of the IPM motor between 0° and 10° is given in figure 3. The peak value of the cogging torque is 2.14Nm, which occurs at about 1.5 mechanical degrees, and not half of 5 mechanical degrees.
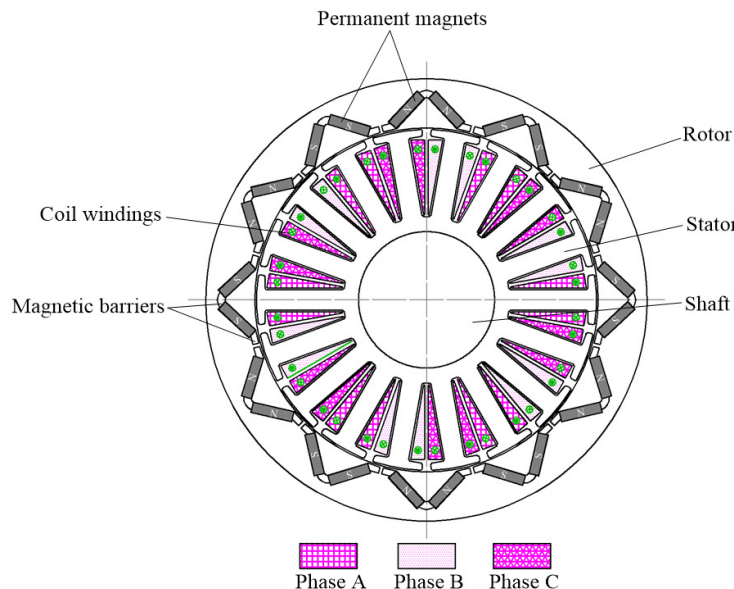
Figure 1. A cross-sectional view of an exterior-rotor IPM synchronous motor.

The discrepancy of the peak position is mainly caused by the salient effects of the salient poles of the IPM synchronous motor. We set the total volume of permanent magnets of each design case as identical for comparison purposes. Figure 4 shows the cogging torque versus the magnet span angle α of the rotor. It is noted that with an increase of the magnet span angle, the peak value of the cogging torque increase. Figure 5 shows the cogging torque versus the shoe depth d_1 of the stator. It can be seen that the peak values of the cogging torque decrease with the increase of the shoe depth. Influences of the shoe ramp d_2 of the stator on the cogging torque are shown in figure 6. It is interesting to find that the peak values of the cogging torque decrease with the increase of the shoe ramp. The cogging torque can be expressed by the integration of the normal and tangential magnetic flux components within the air gap [6]. Because the normal and tangential magnetic flux components within the air gap vary with the geometry shape of pole shoes of the stator, the reduction of the cogging torque can be achieved by modifying pole shoes. By selecting the magnet span angle

α=80°, the shoe depth d_1=4mm and the shoe ramp d_2=30°, the peak value of the cogging torque reduces to 1.05Nm, which decreases 50% in comparison with that of the original design shown in table 1.
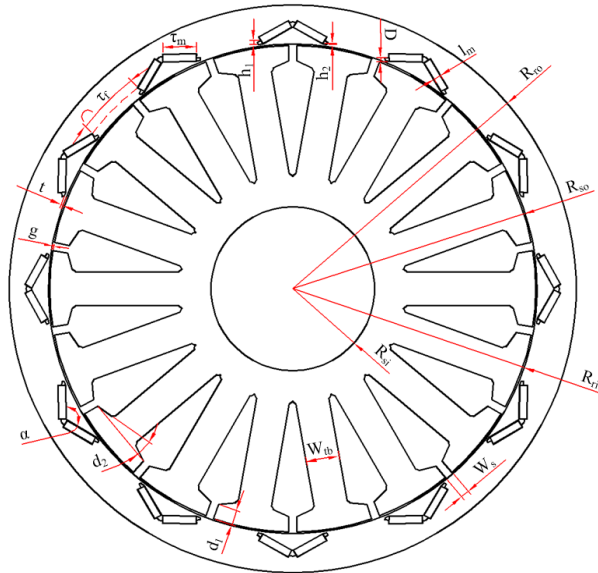
Figure 2. Geometric parameters of an exterior-rotor IPM synchronous motor.

Table 1. Specifications of an exterior-rotor IPM synchronous motor.

NdFeB magnet properties (BNP 12)		
Items	Symbol	Values
Remanence (T)	B_r	0.76
Relative permeability	μ_r	1.26
Direction of magnetization	--	Parallel
Magnet thickness (mm)	l_m	6
Magnet width (mm)	τ_m	24.5
Width between two magnets (mm)	τ_f	10.95
Motor parameters		
Items	Symbol	Values
Number of phases	N_{ph}	3
Number of magnet poles	P	12
Number of armature slots	S	18
Air gap length (mm)	g	1
Slot opening arc (degree)	W_s	3
Outer radius of rotor (mm)	R_{ro}	134
Inner radius of rotor (mm)	R_{ri}	101
Outer radius of stator (mm)	R_{so}	100
Inner radius of stator (mm)	R_{si}	40
Bridge width (mm)	t	1
Air barrier length 1 (mm)	h_1	3.75
Air barrier length 2 (mm)	h_2	1.38
Air barrier width (mm)	D	2
magnet span angle (degree)	α	90
shoe depth (mm)	d_1	2
shoe ramp (degree)	d_2	0
Tooth width of stator	w_{tb}	12
Stack length (mm)	L	25
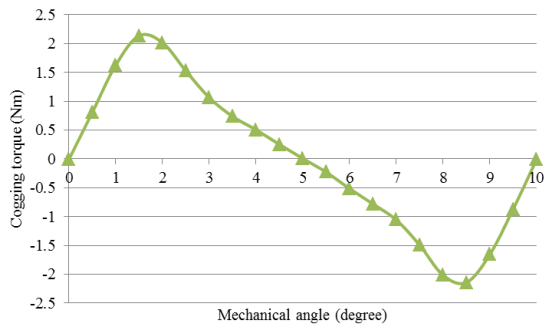
Figure 3. Cogging torque distribution of the IPM synchronous motor shown in figure 1. (α=90°, d_1= 2mm and d_2=0°)
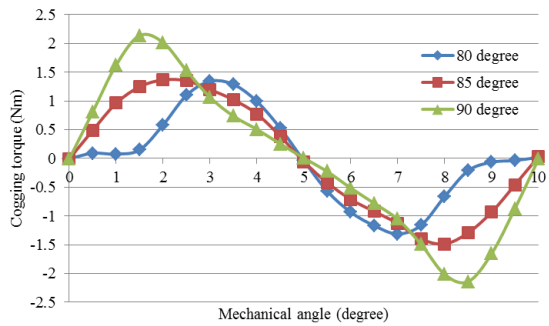
Figure 4. Cogging torque versus the magnet span angle α of the rotor.
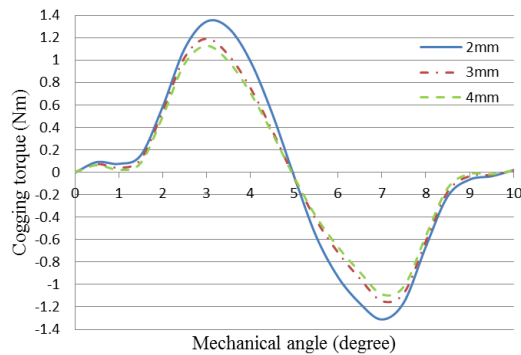
Figure 5. Cogging torque versus the shoe depth d_1 of the stator.
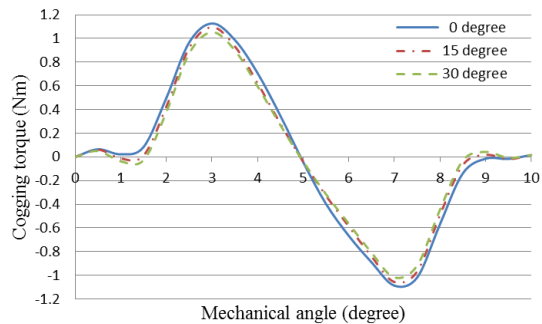
Figure 6. Cogging torque versus the shoe ramp d_2 of the stator.

4. Conclusion

In this paper, the reduction of the cogging torque for an exterior-rotor IPM synchronous motor has been presented by modifying pole shoes of the stator and adjusting the magnet span angle of the rotor. The proposed approach can also be applied for the cogging torque reduction of other permanent-magnet motors with interior-rotor or exterior-rotor configurations.

References

[1] Wang D, Wang X and Jung S Y 2013 *IEEE Trans. Magn.* **49** 2295
[2] Jahns T M and Soong W L 1996 *IEEE Trans. Ind. Electron.* **43** 321
[3] Li T and Slemon G 1988 *IEEE Trans. Magn.* **24** 2901
[4] Eom J B, Hwang S M, Kim T J, Jeong W B and Kang B S 2001 *J. Magn. Magn. Mater.* **226** 1229
[5] Ishikawa T and Slemon G R 1993 *IEEE Trans. Magn.* **29** 2028
[6] Lin Y K, Hu Y N, Lin T K, Lin H N, Chang Y H, Chen C Y, Wang S J and Ying T F 2000 *J. Magn. Magn. Mater.* **209** 180